DOE/PC/91305--4

DE-FG22-91PC91305-4

DE93 009658

# CHARACTERIZATION OF POROSITY VIA SECONDARY REACTIONS

J.M. Calo (Principal Investigator), L. Zhang, and W.D. Lilly

Division of Engineering
BROWN UNIVERSITY
Providence, Rhode Island 02912

Quarterly Technical Progress Report
15 June 1992 - 30 September 1992

Prepared for:
U.S. DEPARTMENT OF ENERGY
Pittsburgh Energy Technology Center
Pittsburgh, Pennsylvania 15236

["US/DOE Patent Clearance is not required prior to the publication of this document."]

## Disclaimer

## SUMMARY

In this quarterly technical progress report, we summarize the progress which has been achieved with the new experimental apparatus currently under development.

**In particular, the following was accomplished during the reporting period:**

- The new TPD-MS/TGA system continues to be tested and improved.
- The focus of the work was on resolving three important problems:

  (1) Improved control of of the temperature programming to minimize large -scale temperature oscillations in the low temperature regime, and flattening out of the temperature response at high temperatures.

  (2) Noise problems with random mass signal fluctuations observed at high temperatures.

  (3) Apparent variation of the sample mass with temperature due to changes in the drag force on the sample bucket.
- The preceding problems have all been addressed, and if not completely resolved, at least minimized to the point where the desorption data are not affected.

**Plans for the next reporting period include:**

- Continued work along the two-pronged mode of attack involving the TPD-MS/TGA experimental system, and the analysis of scattering data to obtain porosity characteristics of coal chars:

  (1) Desorption data will be with the apparatus obtained using char samples oxidized in either $O_2$, $CO_2$ or $H_2O$.

  (2) Work will continue on application of the nonlinear, multiparameter estimation program, to optimize the model parameters used to describe the porosity from small angle scattering data.

# 1.0. PROJECT BACKGROUND

## *1.1. Overview.*

Specific surface area, as well as its accessibility to gaseous reactants, are of paramount importance for all heterogeneous interactions occurring at coal char surfaces. Accessibility of this surface area is governed by the pore structure morphology of the char; i.e., pore size distribution, tortuosity, intersections, shape, etc. The porosity morphology of coal chars varies over a considerable range and is determined by a large number of factors including the nature of the porosity of the precursor material prior to carbonization, the carbonization process, and extent and method of any subsequent activation or gasification. A persistent problem in this area has been the reliable, quantitative measurement and characterization of the resultant porosity, especially the micropores. For example, electron microscopy tends to be qualitative; small angle X-ray or small angle neutron scattering (SAXS/SANS) can suffer from sensitivity to interpretive models, and the inability to distinguish porosity that communicates with the surface from that which does not; and gas adsorption techniques also have several well known drawbacks. The latter, however, are perhaps the most reliable in general, but yield pore size distributions indirectly *via* surface area and pore volume measurements, and can also be laborious and time-consuming. Therefore, there is still a critical need for practical and facile techniques to characterize the porosity of coal chars.

## *1.2. The Current Project.*

The current project is directed at the development of a new approach to this very old problem. During the course of recent work applying temperature programmed desorption (TPD) to the determination of energetic distributions of oxygen complexes on the surfaces of oxidized coal chars (Calo *et al.*, DE-AC21-MC23284), we discovered that secondary interactions occurring within the char

structure during TPD produce characteristic features in the resultant spectra that appear to be quite sensitive to char porosity. The relative and absolute extents of these secondary interactions form the basis of a potential characterization technique. The use of such a method to characterize coal char porosity is potentially attractive because the requisite spectra can be obtained in a single TPD experiment -- a very facile experimental procedure. However, the unambiguous and quantitative interpretation of such data in terms of parameters that can be used to characterize coal char porosity still requires development and an improved understanding of the controlling phenomena. These issues define the primary focus of the current work.

The background and general approach of the secondary interaction method for the characterization of porosity was outlined in the first quarterly technical progress report on this grant (DE-FG22-91PC91305-1), and, therefore, it will not be repeated here. Here we report on the progress that has been made in the construction, development and testing of a new TPD-MS/TGA system being developed in our laboratory for the purpose of conducting the temperature programmed desorption experiments for obtaining the secondary interaction data.

The project plan also includes the use of other techniques to characterize porosity in addition to the secondary interaction approach for the purposes of comparison, quantification, and validation. It is noted that at least two other more well established methods will be used in such a manner. Specifically, gas adsorption techniques in our own laboratory, and small angle scattering (SAS) (X-ray (SAXS) and, possibly, neutron (SANS)). The latter will be accomplished in conjunction with Dr. Peter J. Hall of the Department of Pure and Applied Chemistry of the University of Strathclyde, Glasgow, Scotland. It is planned to obtain small angle X-ray scattering data on the coal chars that will be used in our project *via* access to a small angle X-ray scattering system available in his department. As currently envisioned, Dr. Hall and his co-workers will obtain the X-ray scattering data, and we will analyze these data using models and computational techniques being developed in our laboratory.

## 2.0. PROJECT WORK

### *2.1. The New TPD-MS/TGA System.*

#### *2.1-1. Overview.*

All our past work on thermal desorption of oxygen surface complexes from coal chars was conducted in a TPD reactor apparatus separate from the TGA system (Cahn Model 113) in which the chars were prepared (e.g., see Calo *et al.*, 1989). This procedure was found to work quite well for most of the types of studies that were previously conducted. However, in the current project it is essential to obtain quantitative data of a higher precision than previously in order to develop and validate the *secondary interaction* approach.

In order to meet these requirements, a new TPD-MS/TGA system was designed. A schematic of this system is presented in Figure 1. As shown, this system is built around a new Cahn D-200 digital recording microbalance, which was purchased for this purpose. The TPD reactor is the "hangdown" tube for the microbalance. The system can operate under vacuum conditions to atmospheric pressure, and, most importantly, the coal char sample need never be handled and exposed to undesirable conditions, such as the ambient atmosphere.

A new "clamshell-type" furnace with low "thermal capacitance" was constructed in our laboratory for this system which allows heating to 1100°C, at rates as high as 200K/min. The "clamshell" outer enclosure permits facile access to the hangdown tube for sample loading and removal.

Control and data logging of this experimental system are performed using a Macintosh II microcomputer with a GW Instruments 625 Jr. interface. All the control software has been written in QuickBASIC™.

The entire system has been operational for a few months now, and has undergone extensive testing. However, some "bugs" still remain, which are being resolved. These are discussed below.

### *2.1-2. Work on the TPD-MS/TGA System.*

#### *2.1-2.1 Temperature Variability and Noise.*

The original temperature control system consisted of a built-in routine in the QuickBasic™ program used to control the microbalance and the mass spectrometer. This routine used simple "on-off" control based upon a continuously updated setpoint value according to the preset temperature program. This simple approach was initially applied to the new system, since it worked reasonably well in the predecessor TPD reactor. However, in the new, smaller TPD-MS/TGA apparatus, this technique created some significant problems that had to be addressed. These are presented and discussed in the current section.

Temperature fluctuations and heating rate variations directly affect the mass spectrometer signals during TPD by varying the desorption rate. Figure 2(a) shows an example of "noise" superimposed on the principal CO desorption peak, while Figure 2(b) shows a similar spectrum obtained after improving the temperature programming system to minimize this problem. Also, as shown in Figure 3, the sample mass output signal closely echoes variations in temperature as well. It is of paramount importance to improve the control of the furnace temperature to minimize these effects. Moreover, it is desirable from the point of view of simplifying the analysis and interpretation of TPD data that the heating rate be kept as close to linear as possible.

The principal problems created by controlling the heating rate using the original simple control scheme are temperature "overshoot" in the low temperature region (<400°C), high frequency of furnace cycling in the high temperature region, and leveling-off of the temperature before it reaches its programmed upper limit. The nature and effect of small-scale temperature oscillations at high temperatures have already been demonstrated in Figure 2(a). Figure 4(a) presents some typical results which demonstrate the other two problems. Using the current controller/autotransformer system, in order to attain the ultimate programmed

temperature (typically *ca.* 1050°C), requires a certain minimum output voltage to the furnace. However, the larger the initial voltage setting, the more serious become the oscillations in the low temperature regime due to "overshoot."

The following steps have been taken to overcome or at least reduce these problems to an acceptable level:

(1) The temporary glass wool blanket insulation used on the external surfaces of the furnace has been replaced with a permanent structure made of "wet-wrap" insulating material. The aim was to improve the thermal insulation and insure that the insulation was always the same so that temperature programming could be accurately reproduced from ruin-to-run. This also allows the attainment of ultimate programmed temperatures at lower autotransformer voltages.

(2) An Omega temperature controller has been incorporated to control the power output from the autotransformer output in a "time-proportional" mode. As discussed in previous reports, the heating rate was originally regulated using simple "on-off": control provided by the control program running on the Macintosh IIcx microcomputer. The Omega temperature controller has improved the temperature response of the furnace and reduced the low temperature "overshoot" oscillations.

(3) Rather than attempting to execute the entire temperature program at one pre-set voltage output, a strategy whereby the output voltage is increased once during the run has been adopted. A lower load used in the low temperature region minimizes temperature "overshoot," and a higher load at higher temperatures avoids premature leveling off of the temperature before attaining its ultimate programmed value.

Incorporation of these three strategies has improved the temperature response significantly. Figure 4(b) presents a typical temperature history obtained at a heating rate of 50K/min after the preceding changes were adopted. In comparison to Figure 4(a), it shows less oscillatory behavior at low temperatures and no leveling-off at high temperatures. Also, Figure 2(b) has already shown the improvement in the induced "noise" problem on TPD spectra realized as a result of these actions.

### *2.1-2.2. Apparent Mass Variation With Temperature.*

In the previous technical quarterly progress report (DE-FG22-91PC91305-3), problems associated with convective and buoyancy effects in the microbalance hangdown tube were introduced and addressed. In order to have a large dynamic range in heating rate, the thermal capacitance of the hangdown tube must be kept as low as possible. For this reason, it was decided to use a small diameter quartz tube; i.e., 19 mm O.D., 17 mm I.D. However, in order to maintain this advantage and still work with a reasonably sized sample, the sample bucket must be of a diameter that is on the order of that of the hangdown tube. This gives rise to effects that create an apparent mass variation with temperature as the forces on the sample bucket vary with temperature during the thermal desorption history. This problem has proven to be an important and, unfortunately, persistent one, which appears to have been finally resolved.

The first remedial action taken to minimize these problems was the adoption of a smaller diameter quartz sample bucket (approximately 7 mm in diameter). This eliminated the unacceptably high noise level problems, caused by collisions with the tube walls under certain conditions, and reduced the magnitude of the apparent variation in mass with temperature. However, the latter problems were reduced, but not completely eliminated.

The approach of correcting for these effects by subtraction of the mass behavior of the empty sample bucket under a thermal desorption temperature history (i.e., a "blank" experiment) has been found to be not entirely satisfactory. While this approach seems to work nearly perfectly for an empty sample bucket under "no-flow" conditions, our tests have shown that the apparent mass variation is a function of sweep gas flow rate and species, and sample mass, as well as the primary variable, temperature. While the gas conditions can be well controlled, the sample mass, of course, must vary during the course of an experiment. Consequently,.we have begun to implement an alternate approach that continuously corrects the sample mass during thermal desorption for the drag force due to the

sweep gas flow.

The sample bucket actually behaves as a submerged object in a freely flowing stream. The net force on the sample bucket in the vertical (downward) direction is given by:

$$F_t = F_{drag} - F_b \qquad [1]$$

where:

$F_t$ = net force in the downward direction

$F_b$ = upward buoyant force

$F_{drag}$ = downward drag force on the sample bucket

As it so happens, due to the low density of helium, which is commonly used as the sweep gas, and its low pressure, the upward force due to buoyancy is negligible under typical sweep gas flow conditions. Also, for typical experimental conditions, the free stream flow in the hangdown tube above the sample is laminar; i.e., the Reynolds number (based on the diameter of the hangdown tube, $D_t$, and the free stream velocity of the sweep gas in the tube above the sample bucket, $v_\infty$), $N_{Re} < 1$. This leaves the total drag force as the principal determinant of the apparent mass variation with temperature. Since the feed volumetric flow rate of sweep gas at ambient temperature is kept constant during an experimental run, the linear velocity in the sample tube increases linearly with temperature. This causes the downward drag force to increase during the run, resulting in the predominant apparent mass increase with temperature. At low enough flow rates, and under "no-flow" conditions, a free convective secondary flow has also been observed to develop due to the large temperature gradients imposed by the furnace during the temperature program. This appears to be primarily in the upward direction, and, consequently, leads to an apparent mass decrease. The latter problem is most simply solved by employing a sufficiently high gas flow rate.

While the theoretical determination of the drag force for creeping flow around a sphere is a classic problem, the shape of the sample bucket is a more complex; it has essentially a conical shape with a blunt top (see Figure 5), for which simple theoretical results are not available. However, it is known that the total drag coefficient of a circular disk placed perpendicular to a free flowing stream, is the same as that of a sphere under laminar flow conditions, when referenced to the projected surface area of the sphere; i.e, $C_D = 24/N_{Re}$. (Bird *et al.*, 1960, p. 192). While in the case of the sphere under Stokes or creeping flow conditions the entire drag is due to frictional losses, in the case of the disk there may be an important component of form drag. Therefore, it was decided to assume that the leading, open mouth of the sample bucket approximates a blunt disk, for which $C_D = 24/N_{Re}$. The resultant drag force is given by:

$$F_{drag} = C_D (\pi/4) D_t^2 (1/2) \rho v_\infty^2 = 3 \pi D_t \mu v_\infty \qquad [2]$$

To this can be added the frictional drag associated with creeping flow over the exterior conical face of the sample bucket.

In the latter case, the flow situation is similar to laminar flow in an annulus of continuously varying inner radius. For laminar flow in an annulus of outer radius R and inner radius $\kappa R$ ($\kappa < 1$), the shear stress at the inner wall is given by (Bird *et al.*, 1960, p. 53):

$$\tau_{i.w.} = [4 Q \mu / \pi R^3] g(\kappa), \qquad [3]$$

where: Q is the volumetric flowrate of the sweep gas; R is the radius of the outer wall of the annulus -- i.e., the radius of the hangdown tube, which is constant; and

$$g(\kappa) = [\kappa - (1 - \kappa^2)/(2 \ln(1/\kappa)/\kappa]/[1 - \kappa^4 - (1 - \kappa^2)2/\ln(1/\kappa)] \qquad [4]$$

The differential force exerted on a differential length, dz, of the inner wall is then given by:

$$dF = - \tau_{i.w.} \, 2\pi \, \kappa \, R \, dz \qquad [5]$$

For steady flow, $Q = \pi R^2 v_\infty$, and substituting Eq. [3] into Eq. [5] finally yields:

$$dF = 2\pi D_t \mu v_\infty f(\kappa) \, dz \qquad [6]$$

where:

$$f(\kappa) = [(1 - \kappa^2)/(2 \ln(1/\kappa) - \kappa^2]/[1 - \kappa^4 - (1 - \kappa^2)2/\ln(1/\kappa)]D_t. \qquad [7]$$

The drag force on the lower conical section due to friction in creeping flow is then:

$$F = 2\pi D_t \mu v_\infty \int_0^H f(\kappa) \, dz, \qquad [8]$$

where H is the height of the sample bucket. Numerical integration of the integral in Eq. [8] for H = 0.01 m yields $\int_0^H f(\kappa) \, dz = 0.52$, and thus Eq. [8] becomes:

$$F = 1.04 \, \pi \, D_t \mu \, v_\infty \qquad [9]$$

It is noted that this expression is in the exact same form as Eq. [2], and thus the total drag force on the sample bucket is always of the form:

$$F = n \, \pi \, D_t \mu \, v_\infty \qquad [10]$$

where n is a constant coefficient that depends on the assumptions made concerning the details of the various contributions to the drag force. In any case, the functionality, $F \alpha D_t \mu v_\infty$ is clear. Both $\mu$ and $v_\infty$ are functions of temperature. The variation of the viscosity of helium with temperature is practically linear over the

temperature range of interest (Perry, 1963, p. 3-196), and can be adequately described by:

$$\mu = (1.0816 \times 10^{-2} + 3.303 \times 10^{-5}\, T),\ cp \qquad [11]$$

and

$$v_\infty = (T/T_0)\, v_{\infty,0} \qquad [12]$$

assuming ideal gas behavior.

The resultant correction strategy that suggests itself from this analysis is as follows. First, the mass of the sample bucket under zero flow conditions is "tared" to zero. Then the resultant force acting on the sample bucket at initial conditions of temperature $T_0$ and helium sweep gas velocity $v_{\infty,0}$ is:

$$F_0 = n\, \pi\, D_t\, \mu_0\, v_{\infty,0} \qquad [13]$$

Thus, the difference between the downward drag force at any temperature T and that at the initial conditions is:

$$\Delta F = F - F_0 = n\, \pi\, D\, \mu\, v_\infty - F_0 \qquad [14]$$

Substituting Eqns. [11], [12], and [13] into Eq.[14] yields:

$$\Delta F = F_0\, [(1.0816 \times 10^{-2} + 3.303 \times 10^{-5}\, T)\, T\, /(T_0\, \mu_0) - 1] \qquad [15]$$

where T and $T_0$ are given in terms of absolute temperature, and $\mu_0$ in centipoise.

Since the initial force, $F_0$, can be directly determined at the inception of the run (i.e., it is the mass offset from the "tared" weight of the sample under flow conditions at $T_0$), Eq. [15] can be used to correct for the total force acting on the sample bucket due to the flow of the helium sweep gas as a function of temperature

during the heating process. Figure 6 presents a comparison between experimental results obtained for the apparent mass of the empty quartz sample bucket and the calculated result using Eq. [15]. As shown, the agreement is quite good. This result indicates that this approach to the correction of the sample mass as a function of temperature is promising, and, consequently, will be incorporated into the experimental technique.

## 2.2. *Porosity Characterization Via Small Angle Scattering (SAS).*

### *2.2-1. Overview.*

As indicated above, one of the techniques we are considering for the characterization of coal char porosity is small angle scattering. Although it is well known that these methods are inherently model dependent, they are still quite useful in assessing whether experimental observations are consistent with a given model. In addition, a robust analysis that yields realistic values for the model parameters can be used to infer other properties of the porous structure that can be invaluable in assessing other data, such as that provided by gas adsorption techniques, as well as, in the present case, secondary interaction data.

To date, the preliminary work that we have conducted concerning the analysis of such data has been done in conjunction with Dr. Peter J. Hall of the Department of Pure and Applied Chemistry of the University of Strathclyde, Glasgow, U.K. In addition to this analytical work, it is anticipated that we will be able to obtain small angle X-ray scattering data on the coal chars that will be used in our project *via* access to a small angle X-ray scattering system available in his department.

### *2.2-2. Modeling Porosity From SAS Data.*

As indicated in previous reports, we have been implementing the Fully Penetrable Polydisperse Spheres (FPPS) model, as proposed by Foster and Jensen

(1990), to characterize porosity of chars as determined from small angle scattering data. Essentially, this model approximates porosity by randomly distributing spheres (e.g., voids) within a material (e.g., the solid phase). The interpenetration of these spheres imparts connectedness to the resultant pore structure. The size of these spheres can be distributed over a finite or infinite size range. When the porosity is multimodal, as it is in many coal chars for example, more than one mode or distribution of spheres may be needed to describe the porosity.

The initial work that has been done in attempting to fit some SANS data on coals to a bimodal model., as well as a complete listing of the program SCATTER were included in a previous quarterly technical progress report (DE-FG22-91PC91305-2). In the preceding technical quarterly progress report (DE-FG22-91PC91305-3), we presented the code developed to obtain the "best fit" model parameters to experimental small angle scattering data using an objective function based on the logarithms of the scattering intensities (Foster and Jensen, 1990):

$$\Phi = \sum_{i=1}^{N} [\ln(I^*(h)) - \ln(I(h))]^2, \qquad [16]$$

where the $I^*(h)$ and the $I(h)$ are the experimental and calculated scattering intensities, respectively. The technique selected for this purpose is the Levenberg-Marquardt, or Marquardt method, which has become the standard for nonlinear least squares routines. This method has been implemented in the code MARQFIT, which was presented in the previous technical quarterly progress report (DE-FG22-91PC91305-3).

The status of this effort remains essentially as described in the previous report since our efforts have been primarily focused on resolving the remaining experimental problems on the TPD-TGA/MS system. The first tests of the data analysis software involve SANS data obtained on certain solvent-swollen Argonne Premium Coal Sample Bank coals at the Argonne National Laboratory by Dr. P.J.

Hall of the University of Strathclyde, and co-workers. The important issues that remain to be resolved are the number of modes necessary to accurately fit the data, and the continued development of an automated parameter estimation technique using a Marquardt-type approach.

## 3.0. PLANS FOR NEXT REPORTING PERIOD

Plans for the next reporting period include continued work along the two-pronged mode of attack involving the TPD-MS/TGA system and the analysis of scattering data to obtain porosity characteristics of coal chars.

The apparatus appears to be at the point where reliable desorption data may be obtained using char samples oxidized in either $O_2$, $CO_2$ or $H_2O$.

Work will continue on application of the nonlinear, multiparameter estimation program, to optimize the model parameters used to describe the porosity from small angle scattering data.

## REFERENCES


Bird, R.B., Stewart, W.E., and Lightfoot, E.N. *Transport Phenomena,* Wiley and Sons, NY, 1960.

Calo, J.M., Hall, P.J., and Lilly, W.D., *A Mechanistic Study of the Energetic Heterogeneity of Coal Chars,* DOE/MC23284-F, DOE-METC Final Technical Report, 1989.

Foster, M.D., and Jensen, K.F., *J. Coll. Intf. Sci.* **135**, 132 (1990).

*Perry's Chemical Engineers' Handbook,* Perry, Chilton, Kirpatrick, eds, Fourth edition, McGraw-Hill, 1963, p. 3-196.

Press, W.H., Flannery, B.P., Teukolsky, S.A., and Ketterling, W.T., *Numerical Recipes - The Art of Scientific Computing,* Cambridge University Press, New York, 1987.

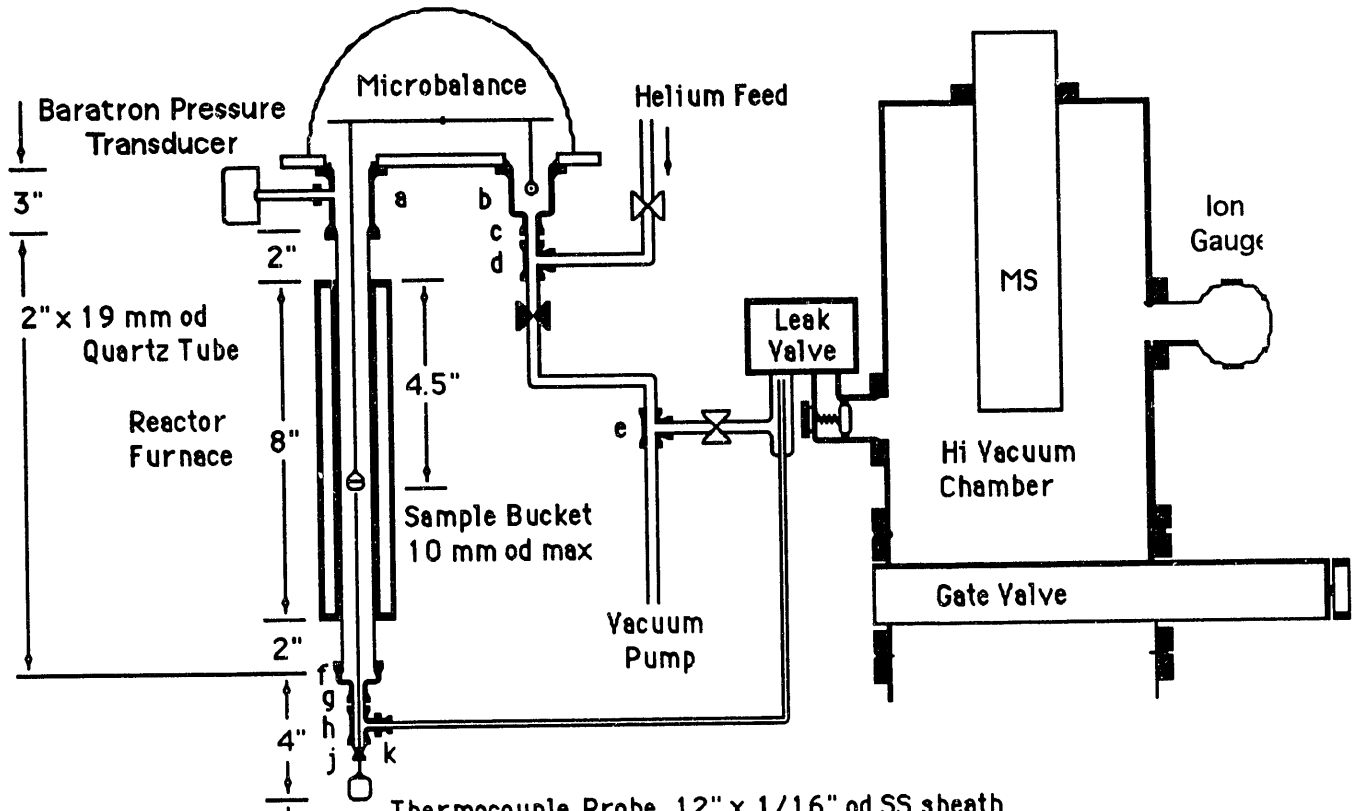


FITTINGS:

| | | |
|---|---|---|
| a | SS-12-UT-A-16* | 1" tube stub to 3/4" Cajon Adapter |
| b | SS-810-R-16 | 1" tube stub to 1/2" Swagelok |
| c | SS-400-R-8 | 1/2" to 1/4" Swagelok Reducer |
| d | SS-400 - 3 | 1/4" Swagelok Tee |
| e | SS-400 - 3 | 1/4" Swagelok Tee |
| f | SS-12 - UT - 6 | 3/4" Cajon Union |
| g | SS-810-6-12 | 3/4" to 1/2" Swagelok Reducing Union |
| h | SS-810-3 | 1/2" Swagelok Tee |
| j | SS-100-R-8 | 1/2" to 1/16" Swagelok Reducer |
| k | SS-200-R-8 | 1/2" to 1/8" Swagelok Reducer |

Figure 1. Schematic of new TPD-MS/TGA apparatus.

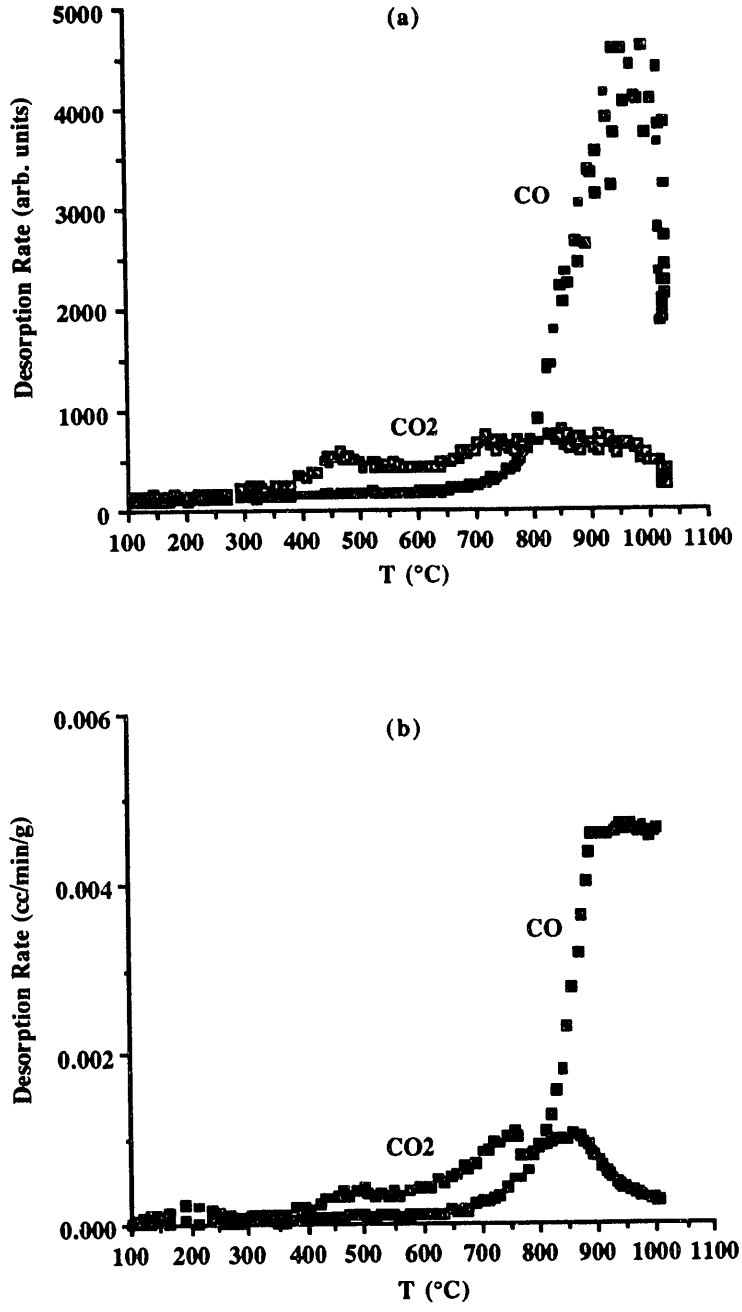


Figure 2. CO and $CO_2$ desorption spectra obtained at a heating rate of 50K/min for Wyodak coal char prepared at 1000°C for 2 h in helium and gasified to 5% burn-off at 800°C in 0.1 MPa of $CO_2$. (a) with; (b) without random noise on the high temperature CO peak.

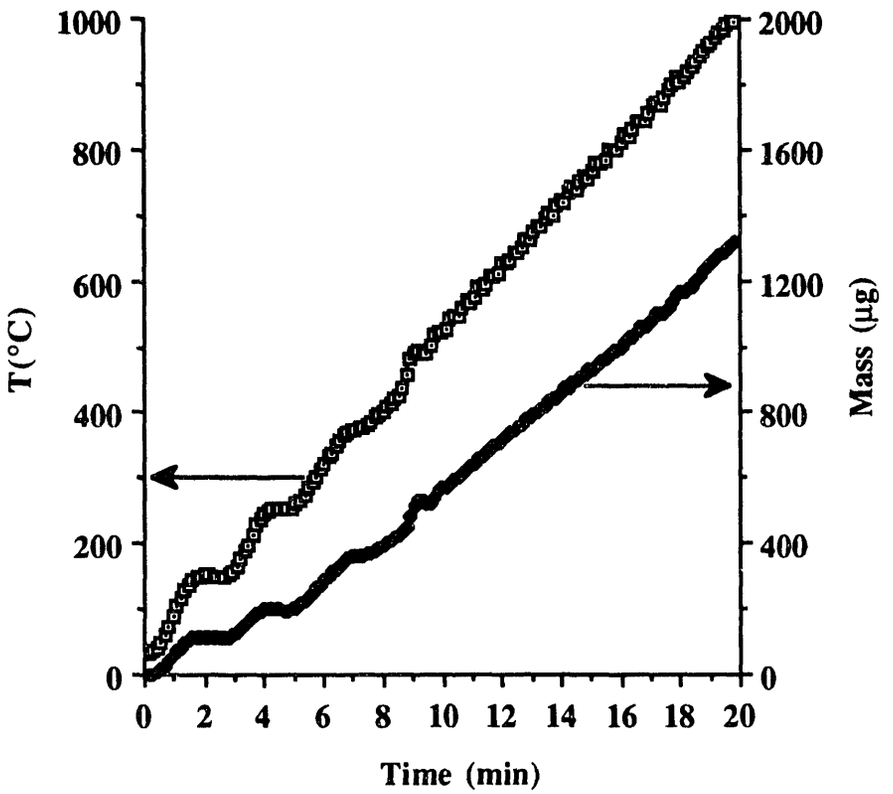


Figure 3. Mass and temperature histories of the empty quartz sample bucket during a heating program at a nominal heating rate of 50K/min.

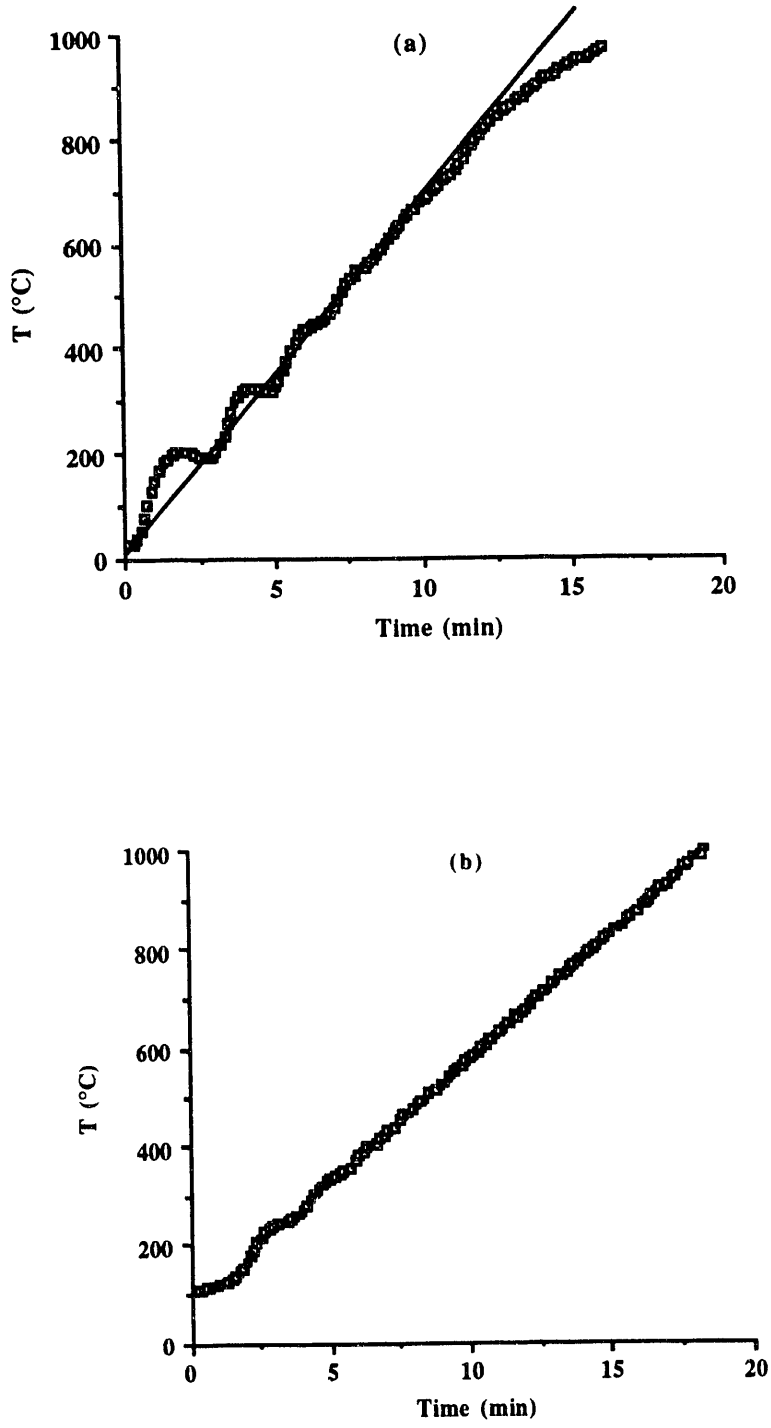


Figure 4. Comparison of increasing temperature programs at a nominal heating rate of 50K/min. (a) original performance; (b) current performance.

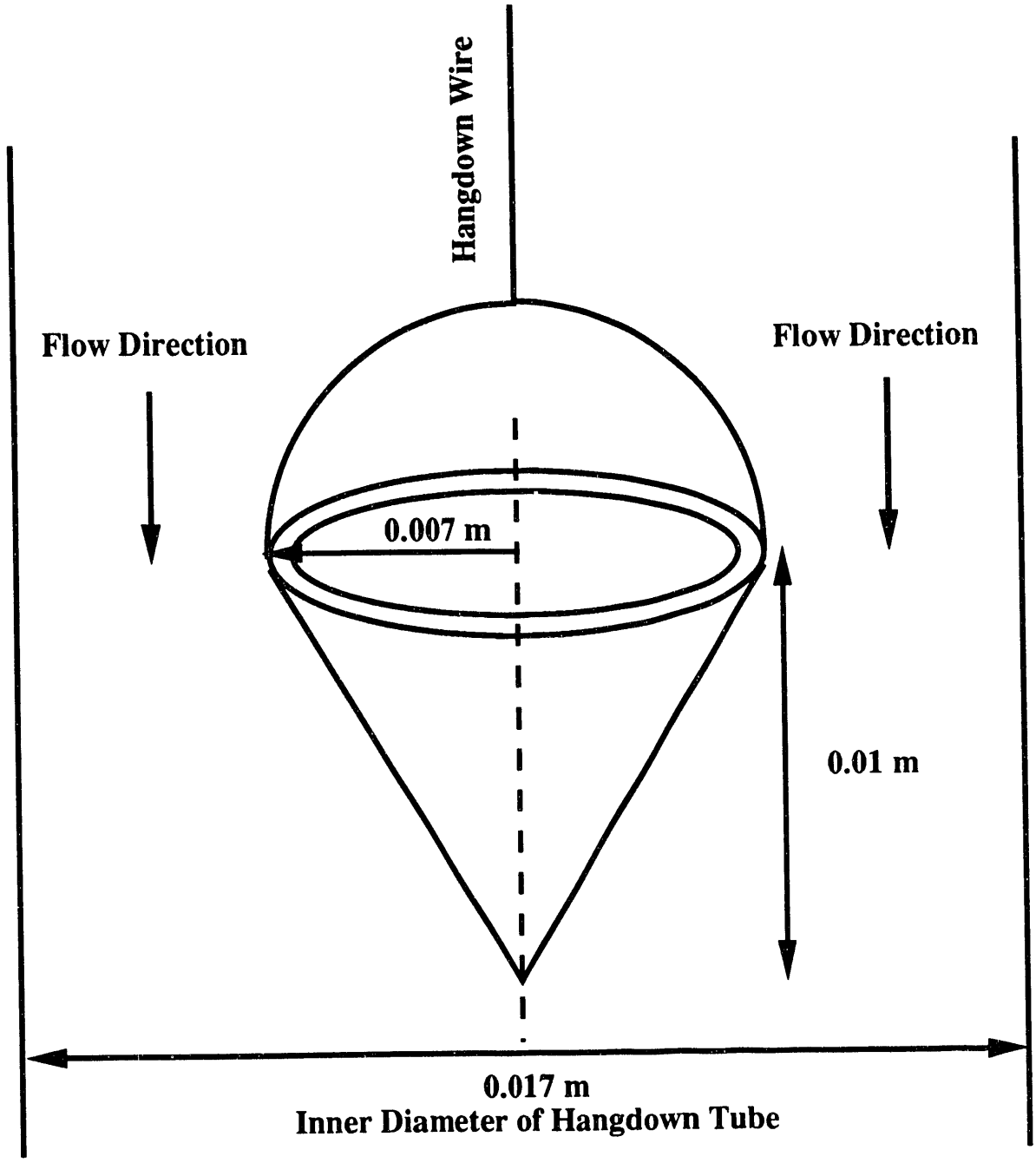


Figure 5. Approximate geometry of the quartz sample bucket.

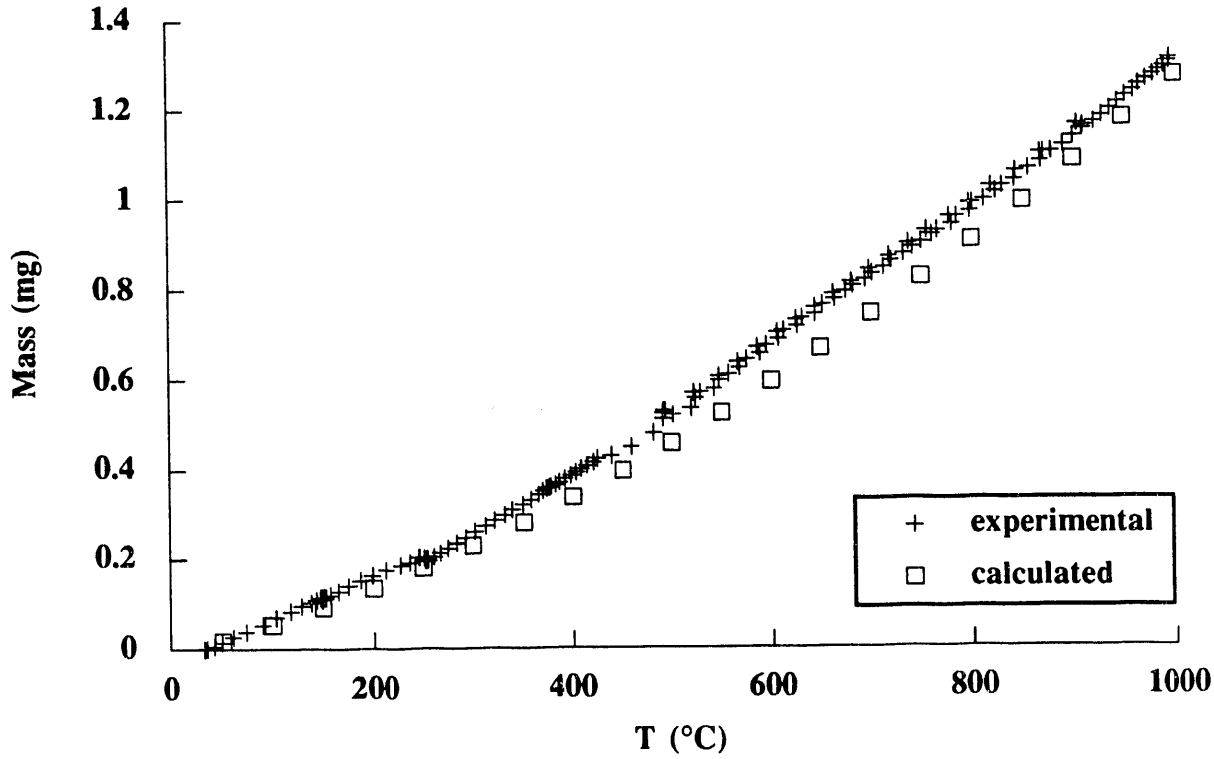


Figure 6. Comparison of observed and calculated apparent mass variation of the empty quartz sample bucket at a heating rate of 50K/min and a helium flowrate of approximately 65 scc/min.

# END

DATE
FILMED
4/11/93